International Journal of Fatigue 164 (2022) 107149

Contents lists available at ScienceDirect

International Journal of Fatigue

journal homepage: www.elsevier.com/locate/ijfatigue

Influence of the ratio between specimen thickness and grain size on the fatigue and tensile properties of plain and notched aluminium plate specimens

P. Lorenzino [a], A. Navarro [b,*]

[a] Constellium Tecnology Center, Parc Economique Centr'alp, CS10027 Voreppe 38341 Cedex, France
[b] Departamento de Ingeniería Mecánica y Fabricación, Escuela Superior de Ingenieros, Universidad de Sevilla, Camino de los Descubrimientos s/n, 41092 Sevilla, Spain

ARTICLE INFO

Keywords:
Aluminium
Thickness effects
Size effects
Grain size
Mechanical properties
Hall–Petch relation
Notch sensitivity

ABSTRACT

The influence of the ratio between specimen thickness (t) and grain size (D) on the tensile and fatigue properties of plain and notched aluminium plate specimens has been studied. Grain sizes ranging from 66 μm to 9.74 mm have been prepared and used in the tests. The observed decrease on tensile properties when D is comparable, or even exceeds, t can be accounted for by adding an additional negative exponential term to the Hall–Petch equation. An exponential decrease has also been found in endurance limits as grain size approaches plate thickness in *plain* specimens. In *notched specimens*, however, increasing grain size has two opposing effects, namely: a decrease in the plain endurance limit associated with the decrease in thickness relative to grain size and an increase in notched fatigue strengths brought about by a decrease in notch sensitivity.

1. Introduction

A particularly challenging problem in certain specialized applications is the assessment of the fatigue strength of components that are very small compared with the standard specimens used to obtain mechanical and material properties in normal laboratory practice. This raises the question of whether those material data, for example the plain fatigue limit, obtained in the standard way may be appropriate or useful for the fatigue design of such small pieces.

For example, the stents used in coronary angioplasty are small wire mesh tubes, the framework of which is made of thin struts interlaced to form a kind of chain link fence with a pattern of variously shaped cells, depending on the manufacturer, with sides one or two millimeters long. Stent failure by fatigue is increasingly recognized as a major cause of concern, with potentially important clinical consequences [1]. Thus, the US Food and Drug Administration (FDA) [2, p. 19] indicates that "Failure of a stent due to fatigue may result in loss of radial support of the stented vessel, thrombus formation or focal restenosis, or in perforation of the vessel by the stent struts. Fatigue analysis, combined with stress/strain analysis and accelerated durability testing, provides an indication of device durability". The FDA even recommends that "you determine the fatigue resistance of the stent to physiologic loading using a Goodman analysis or another fatigue life analysis method". Ten years of durability data is deemed to provide sufficient proof of safety of the device for the majority patients [2, p. 20], which corresponds to around 4 $\times 10^8$ systolic–diastolic cycles [3], well within the high cycle fatigue regime. The width and thickness of the struts are about 100 to 150 μm. With typical grain sizes of around 10 to 30 μm for the stainless steels and cobalt chromium alloys [4] used (among other materials) in their manufacture, the small number of grains in the cross section makes the application of models based on standard bulk properties rather questionable [5,6]. This is then an example where the use of macroscopic or bulk material properties might be inappropriate and where an improved knowledge of baseline mechanical properties of the material when relevant component dimensions are comparable with the microstructural grain size would be desirable.

Models based on crystal plasticity and finite elements [7–9], coupled with comprehensive microstructural information [10–12], have been developed for combining the micro and macro scales to predict mechanical performance of components such as those referred to above, where the microstructural size is comparable to the physical size. These models and experimental procedures are extremely useful with a view to understanding the fundamental aspects of the mechanisms governing mechanical properties. However, they are less useful for dimensioning components at the engineering design stage, where only general properties of the material are considered.

* Corresponding author.
E-mail addresses: pablo.lorenzino@constellium.com (P. Lorenzino), navarro@us.es (A. Navarro).

https://doi.org/10.1016/j.ijfatigue.2022.107149
Received 6 April 2022; Received in revised form 8 July 2022; Accepted 13 July 2022
Available online 22 July 2022

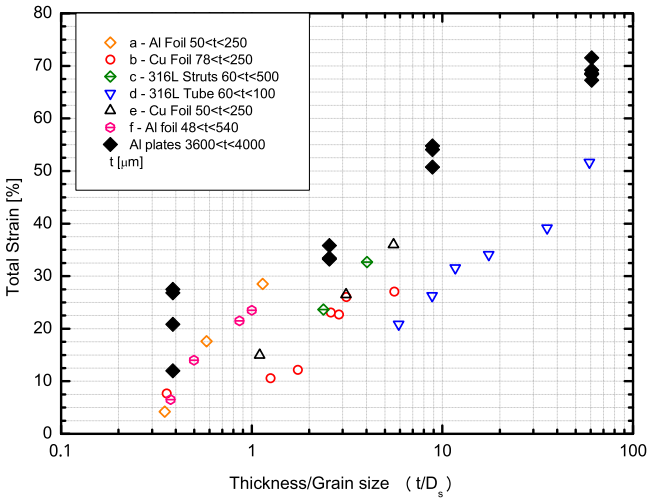

Fig. 1. Variation of fracture strain as a function of the ratio between specimen thickness and surface grain size, t/D_s. Data from our own experiments with aluminium plates of thickness between 3.6 and 4.0 mm and from the following sources: (a) and (b) [13,14]; (c) [15]; (d) [16]; (e) [17] and (f) [18].

Dimensional analysis arguments suggest that the ratio between the thickness and the grain size may be of some help here. Fig. 1 shows the fracture strain as a function of the ratio between specimen thickness and grain size taken from several studies. It also shows data from our own experiments with plates of thickness between 3.6 and 4.0 mm. Although our specimens are much thicker than those shown from the other authors, they span the same range for the t/D_s ratio (since we are using unusually large grains, see below). Here, D_s is the grain size measured on the specimen large planar free surfaces, as opposed to D_t, which is measured across the specimen thickness. D_s and D_t are generally different and both will be used in the discussion below. As can be seen, fracture strain decreases when the t/D_s ratios diminish. Note also how the scatter greatly increases for our own data on the Al plates. This figures gives an early indication that there is a potential effect of lack of constraint in the plastic deformation of the grains, which produces a noticeable drop in the strength of the specimens. This comparison underlines the significance of grain size as compared with the specimen's other dimensions in characterizing the mechanical properties and how such properties can be expected to change with specimen size.

Of course, microstructure has long been known to influence the mechanical properties of materials. The key point here is whether some other parameter, such as the ratio just mentioned, must be brought to bear into the problem when the dimensions of the specimen are comparable to the grain size.

The pioneering work in relating mechanical properties to microstructural size is due to Hall (1951) [19] and Petch (1953) [20] who independently showed that the lower yield stress of poly-crystalline iron obeys an equation of the form

$$\sigma_y = \sigma_0 + k_0 D^{-1/2} \tag{1}$$

They suggested that yielding is caused by the stress concentration due to dislocation pile-ups at grain boundaries. Then, σ_0 represents the friction stress opposing dislocation motion in the pile-ups, k_0 the contribution of grain boundaries to hardening and D the grain size. Later, Conrad and Schoeck [21] showed that in iron the flow stress for a strain beyond the Lüders strain obeyed a similar equation.

This relation has been shown to apply in specimens of dimensions considerably exceeding their microstructural size (i.e., bulk materials) in several studies. Fewer have, however, explored what happens when the dimensions of the specimens (at least one of them) becomes comparable to the grain size. This is most easily done by working with plate specimens whose thickness is progressively reduced while the other dimensions (and the grain size) are kept fixed. An alternative route is to maintain the overall dimensions of the specimens while producing progressively bigger grains with the appropriate thermo-mechanical treatment. This is what we have done here. But, before describing our experiments, let us review some previous results found in the literature.

A pioneering article by Pell-Walpole [22] studied the influence of grain size compared to the overall specimen dimensions on the tensile strength of tin and certain of its alloys. An increase in tensile strength was found as the grain size decreased from 1 to 20–30 grains in the cross-section. Over this range, elongations were constant. Further reduction in grain size produced only a slight increase in tensile strength, but elongation were seen to increase rapidly. The critical grain size associated with this change of behavior corresponded approximately to the first occurrence of completely enclosed grains in the cross-section of the specimen. It was suggested that this change is accompanied by a partial change in the mechanisms of deformation, possibly the occurrence of viscous flow in addition to the normal processes of slipping and twinning.

Later Miyazaki et al. [23], examined the influence of specimen thickness on tensile properties, looking explicitly at the influence of the specimen thickness-to-grain size ratio (t/D). They used 99.994 wt% Al, 99.991 wt% Cu, Cu-13 wt.% Al and Fe films and found their tensile strength to decrease exponentially when t/D values fall below a critical threshold.

In 2005, Janssen et al. [24] followed the previous work of Miyazaki et al. but considered the fact that film grains switch from equiaxial to pancake-shaped when their size is large enough for t/D to fall below 2. They then defined the two different measures of the grain size introduced above, namely: D_s and D_t. In specimens with $D_t \approx t$, crystals have two free surfaces and grain boundaries extend along the whole thickness (i.e., they are sort of "vertical walls" grain boundaries). Janssen et al. developed a hardening (or softening) model based on the ratio between grain boundaries and grains inner zones. The numerical and graphical results of this model are, however, purely qualitative and cannot be used to examine variability in material properties as in the Hall–Petch relation.

Keller and Hug [25–28] studied films of highly pure (99.98 wt%) nickel with variable thickness-to-grain size ratios in order to see whether they conformed to the Hall–Petch relation and found that specimens containing a small number of grains across their thickness depart from it. They concluded that hardening mechanisms – and hence the equation's coefficients – changed when $t/D < 4$, where the stress was much more strongly dependent on grain size. Also, they found the change to be strain-dependent and due to hardening effects. The friction stress σ_0 was found to be smaller than in the case of specimens with a grain size much smaller than their thickness.

Klein et al. [13] examined the strain-stress behavior of copper and aluminium specimens 10 to 250 μm in thickness and 2 to 250 μm in grain size. They identified a size effect that was ascribed to textural differences (viz., differences in the number of active slip systems associated to thickness and grain size) and found the t/D ratio to have a much more marked effect on fracture strain than on stress. Also, they assumed microstructure in materials of grain size similar to or even larger than thickness to be a two-dimensional array of single crystals and, consistent with the low fracture strain levels observed, deformation in the material to occur largely in only one or two slip systems.

In 2001, Fu et al. [29] reported careful, extensive analytical and computational work on the influence of grain size on yield stress, but failed to examine the effect of specimen thickness. By using very small grain sizes – down to the typical dimensions of nanocrystalline materials – relative to specimen thickness, they reached the following conclusions: (1) Grain boundaries acted as barriers against plastic flow (2) Grain boundaries also acted as dislocation sources (3) Elastic anisotropy in the material caused additional stresses around grain

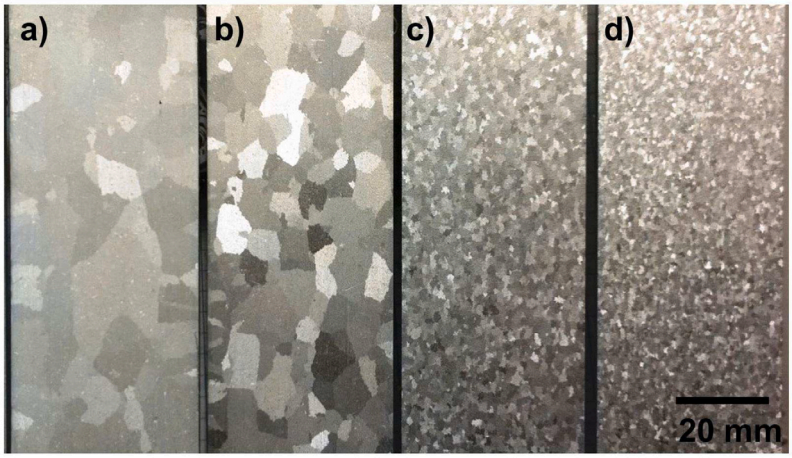

Fig. 2. Microstructural changes in a 2 mm thick specimen upon application of a total deformation of (a) 8%, (b) 10%, (c) 14% and (d) 16%.

boundaries (4) Grain boundaries underwent multiple slip, whereas inner zones slipped in a single direction — the most favorable one. As a result, regions near grain boundaries harden faster than inner regions of the grains.

Recently, Lederer et at. [18,30] reported a comprehensive study of the dependence of mechanical properties on the thickness to grain size ratio over a wide range of variation. They performed tensile tests at room temperature and 100 °Celsius on highly pure (99.999%) aluminium films 5 to 540 μm in thickness, spanning a t/D_s range from 0.0485 to 1, and found a marked effect of grain size on mechanical properties. Thus, the specimens with $t/D_s < 1$ – where the Hall–Petch relation does not hold because most grains are at the free surface – exhibited a decreased tensile strength; they also noticed the presence of an oxide layer on the thinnest films (5-20 μm). They concluded that the mechanical properties of the material were influenced by the combined effect of specimen size, grain size, the presence of an oxide surface layer and the testing (or working) temperature. This precluded extrapolating the results to specimens with considerably greater thicknesses. Zhang et al. [31] reached similar conclusions on fatigue properties.

Two studies by Dai et al. [32] and Simons et al. [33] are also worth mentioning. These authors assessed static and fatigue properties in free-standing copper foils of variable thickness, and found tensile strength and fatigue resistance to decrease with decreasing film thickness.

All the studies described above revealed that the closer the grain size was to some characteristic dimension of the specimen, the stronger was the dependency of its mechanical properties upon grain shape and orientation.

Although there are many contributions studying changes in monotonic mechanical properties with decreasing component dimensions [13,14,17,31,32,34–47], size effects on fatigue properties have been addressed much less frequently. Except for the work of Wiersma and Taylor [48], studies in this area have focused on the behavior of plain specimens or on crack propagation in notched components – without addressing notch sensitivity issues in the latter case. No study considering the effect of thickness in notched specimens – which would be quite revealing since most industrial components have some notch or stress concentrator — has to date been reported, to the best of our knowledge. In this work, we conducted a systematic study of the influence of t/D on the fatigue limit of plain and notched components. The latter were examined with provision for the fact that, when grain size approaches specimen thickness, competition arises between the thickness effect — by which the fatigue limit decreases with decreasing thickness-to-grain size ratio and the notch sensitivity effect — by which the limit increases with increasing notch size-to-grain size ratio.

Although the t/D values used here spanned the specimen size range from macro-scaled components to single crystals, there was no need to use specimens of the latter type, as explained below.

2. Experimental procedure

2.1. Material

The primary purpose of this work is to examine the influence of grain size and specimen thickness on the fatigue and tensile behavior of plain and notched aluminium plate specimens. In particular it aims to characterize the point where the mechanical properties start to decline and the material can be consider to behave like a *thin film*, so to speak.

In order to deal with as few unknowns as possible, we used a material consisting of a single-phase metal of easily controlled grain size. Also, in order to span as wide a grain size range as possible, we used commercially pure aluminium alloy 1050 for testing as recommended by Carpenter and Elam [49,50].

2.2. Thermomechanical treatment

Previous work by our group [51–53] revealed that grain size in commercial pure aluminium sheets can be substantially increased by using two thermal treatments immediately followed by cold deformation. The process is very simple and easily controlled, and provides results with very small scatter. In this work, we used 1, 2 and 4 mm thick sheets of aluminium 1050, an alloy consisting of 99.56% Al, 0.08% Cu, 0.2% Fe and 0.1% Si. The sheets were cut into 45 × 200 mm pieces in the lamination direction and thermally treated in a Carbolite 215GHA12 furnace. The first thermal treatment was intended to obtain a strain-free equiaxial structure by heating from room temperature to 550 °C at 2.6 °C/min. The second thermal treatment involved keeping the specimens at 550 °C for 5 h and allowing them to cool in air. Increasing the length of the constant-temperature treatment led to increased growth in surface grains relative to inner grains. The gradient in grain size resulted in non-uniform deformation across the thickness of the specimens in the following step, the mechanical treatment. Grain size after the second recrystallization was governed by the amount of deformation applied during the cold deformation treatment, which differed with thickness (viz., 5, 6, 7, 8, 9, 10, 12, 14, 16 and 18% for the specimens 1 or 2 mm thick; and 8, 11, 14 and 18% for those 4 mm thick). The treatment was performed on an MTS 810 testing machine operating under strain-controlled conditions. The third step of the process involved heating to 550 °C at 2.6 °C/min, holding the final temperature for 15 h, raising it to 575 °C and holding for 1 h, which was followed by air-cooling. This step caused new crystals to form from old ones, the final crystal size depending largely on the amount of plastic deformation applied.

Fig. 2 illustrates the typical microstructures obtained and the total deformation applied to 2 mm thick specimens.

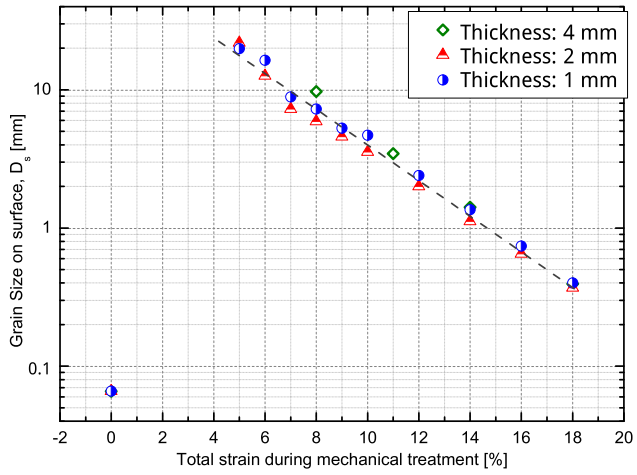

Fig. 3. Variation of surface grain size with the amount of deformation applied during the thermomechanical treatment.

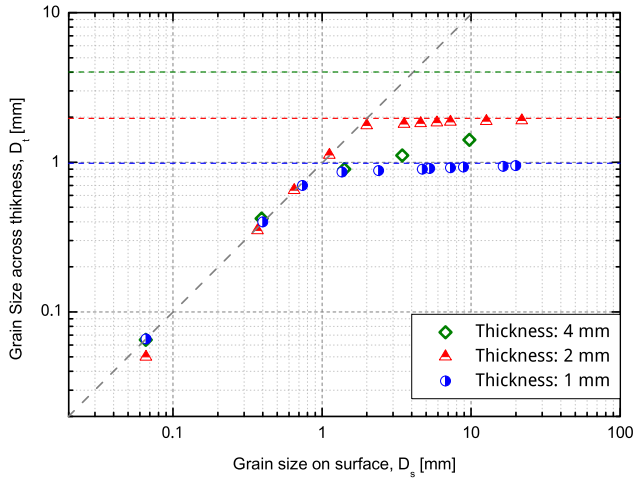

Fig. 4. Variation of grain size in the thickness direction as a function of surface grain size.

2.3. Grain size analysis

Grain size was determined in accordance with ASTM E112, using the software Simagis Live as described elsewhere [51–54]. Fig. 3 shows the variation of the resulting grain size with the amount of deformation applied to specimens of different thicknesses. There is a good correlation between surface grain size and the amount of deformation applied. The isolated dot on bottom-left part of the figure (grain size for 0% of strain) corresponds to the material without any mechanical treatment, having undergone only the first annealing for re-crystallization, resulting in a grain size of around 66 μm for the three thicknesses. As can be seen from Fig. 4, the surface grain size in the 1 and 2 mm thick specimens was comparable to their transverse dimension (i.e., surface grains were equiaxial). When the surface grains grew larger than the specimen thickness, they spanned the whole thickness and formed a two-dimensional array of single crystals. This was not the case with the 4 mm thick specimens, where the mechanical treatment created a strain gradient across the material and led to a layered structure after the second thermal treatment [51]. The number of grains across the thickness of a specimen has a strong influence on its mechanical properties [23,51,52,54].

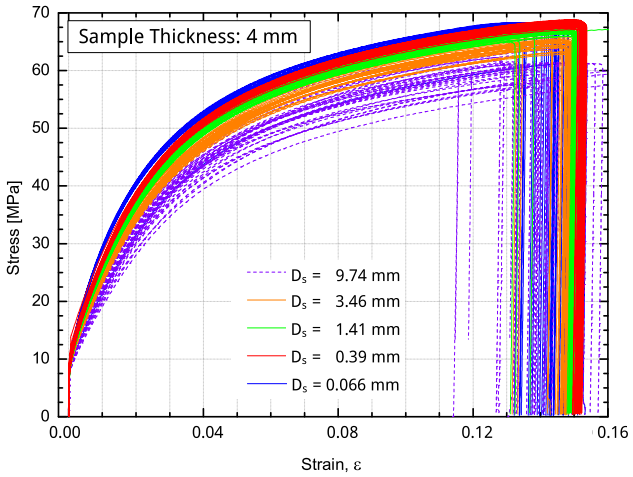

Fig. 5. Stress–strain curves reflecting an increase in tensile strength, as well as a decrease in the spread between the curves for each grain size, with decreasing grain size.

2.4. Tensile and fatigue tests

Tensile tests were performed in an MTS 810 servohydraulic machine operating at 0.2 mm/s under displacement-controlled conditions. Fatigue tests were conducted on a RUMUL Testronic 100 kN resonance machine. All tests were carried out under load-controlled conditions, using R = 0.1 (pull–pull) and peak stress values from 45 to 95 MPa. The resonance frequency for these loading conditions and specimen geometry range from 75 to 90 Hz. As regards failure, crack propagation involves a decrease in the specimen cross-sectional dimension resulting in a decrease in measured resonance frequency [53]. Preliminary testing allowed failure to be associated with a 0.7 Hz decrease in the frequency. A larger decrease signaled the immediate failure of the material: crack sides fell apart and the remaining cross-section underwent plastic deformation, thereby precluding accurate post-mortem analysis.

3. Results and discussion

3.1. Tensile properties

3.1.1. Influence of grain size

Each test specimen had an initial constant gauge geometry of 300 × 45 × 4 mm. The initial cross sectional area changes with the mechanical treatments applied for increasing the grain sizes. Thus the cross sectional area of each specimen depends on the particular mechanical treatment which has been applied to it, ranging between the initial area of 180 mm^2 to 148 mm^2. Fig. 5 shows examples of the stress–strain results obtained for the 4 mm thick specimens. The tensile strength increased with decreasing grain size. Also, scatter increased with increasing grain size. As can be seen in the graph, the spread between the curves belonging to the same grain size decreased with decreasing grain size (see also Fig. 6). Tensile tests were interrupted at 13 to 15% of strain since these specimens would later on be used to perform the fatigue tests. After performing these tensile tests the yield strength ($\sigma_{0.2}$) was increased to a range between 75 and 95 MPa and thus the subsequent fatigue tests were all done in the elastic regime. It should be noted that results shown in Fig. 5 are expressed in terms of engineering stress and not in terms of true stress. However, the cross-sectional area reduction is taken into account when calculating the new yield strength of the specimens used for the fatigue tests.

Scatter in the results was assessed from sections at different strain levels in the stress–strain graphs. Fig. 6 shows the distribution of true stress for a deformation of 5% in samples 4 mm thick. The number of

Table 1
Average true stress and standard deviation at different grain sizes and deformation levels. Samples thickness: 4 mm.

Group	n	D_s [mm]	Strain level											
			0,20%		0,30%		0,50%		1,0%		2,0%		5,0%	
			σ_v [MPa]	Stdv.	σ_v [MPa]	Stdv.	σ_v [MPa]	Stdv.	σ_v [MPa]	Stdv.	σ_v [MPa]	Stdv.	σ_v [MPa]	Stdv.
0%	31	0.066	14.67	0.13	17.01	0.14	21.10	0.16	29.41	0.22	41.20	0.23	58.75	0.19
18%	40	0.39	13.42	0.31	15.50	0.30	19.16	0.29	26.99	0.30	38.97	0.33	57.54	0.35
14%	39	1.41	12.85	0.27	14.77	0.27	18.18	0.27	25.63	0.30	37.35	0.36	55.93	0.37
11%	31	3.46	12.35	0.31	14.10	0.32	17.26	0.39	24.19	0.58	35.43	0.74	53.65	0.79
8%	41	9.74	11.75	0.59	13.28	0.70	16.06	0.88	22.33	1.27	32.81	1.71	50.24	2.13

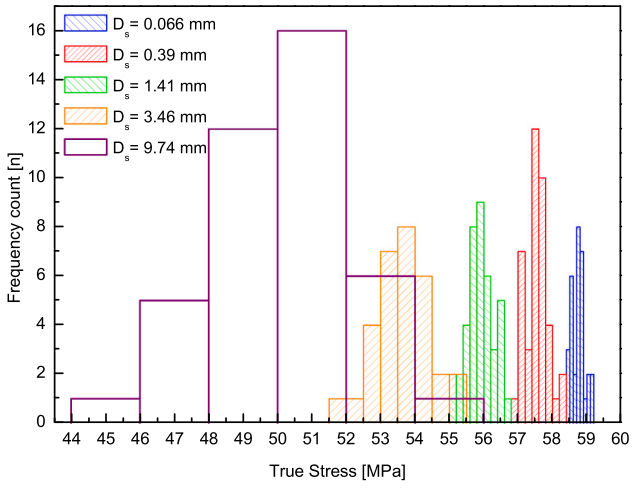

Fig. 6. Stress distribution for an applied deformation of 5%. Samples' thickness: 4 mm. Number of tests performed at each grain size: (a) 41 at 9.74 mm, (b) 31 at 3.46 mm, (c) 39 at 1.41 mm, (d) 35 at 0.39 mm and (d) 31 at 0.066 mm.

tests performed at each grain size were as follows: 41 at 9.74 mm, 31 at 3.46 mm, 39 at 1.41 mm, 35 at 0.39 mm and 31 at 0.066 mm. As in the previous graph, mechanical properties increased and their distribution became narrower with decreasing grain size. Shapiro–Wilks statistical tests were performed in order to check whether the results may be assumed to belong to a population with a Gaussian distribution and this was the case for all the grain sizes.

Table 1 shows the results obtained for different grain sizes and deformation levels. Stresses decreased and their standard deviation increased with increasing grain size. The increased scatter in the curves was a result of a decrease in the amount of grains contained in each specimen and also of the grain size being close to the gauge length of the extensometer used. As a consequence, the amount of deformation was not a global, but rather local, variable dependent on the Schmid factor for the grains where the extensometer was positioned.

3.1.2. Hall-Petch relation

According to Hall–Petch, the mechanical properties of a material increase with decreasing grain size. This is a result of an increased number of grain boundaries, which are responsible for halting dislocations during plastic deformation. The variation of the tensile strength of a material with the reciprocal square root of its grain size is a straight line of positive slope (in log–log coordinates). However, it is well known that the evolution of yield stress in specimens with nanometrically sized grains departs from this linear dependence and tends asymptotically to a plateau defined by the yield stress for grain boundaries themselves [29]. As grain size increases and one moves, so to speak, to the other end of applicability of the Hall–Petch equation, the slope increases [5,25] by effect of the influence of specimen thickness. Based on available data for the influence of thickness irrespective of grain size [23,24], mechanical properties decrease exponentially as the grain size approaches the specimen thickness (viz., at a t/D_s value below 5 or 10 on the stress vs t/D_s graph). This experimental observations are well described by the model proposed by Miyazaki and co-workers that considers that in interior regions of thick specimens, all grains are homogeneously deformed by the strong interaction among grains. In the surface layer, however, the constraining force of individual grains markedly decreases so that only a part of each grain near the boundary is affected by neighboring grains, leading to an exponential decrease in mechanical properties. The radius of the affected zone, in which individual grains strongly interact with each other, is estimated using this simple model. The result shows that the long-range interaction among individual grains expands into a wide region across the first nearest-neighbor grains.

If the influence of thickness on the Hall–Petch relation is considered, a material might be expected to lose mechanical properties in an exponential manner as the grain size approaches the specimen thickness. The resulting Hall–Petch curve would be defined by the well-known linear relation in addition to a term reflecting this exponential decrease beyond a critical grain size threshold dependent on specimen thickness. It should be noted that such a threshold is not unique for each material but rather a function of specimen size. Thus, whether two specimens of the same material having an identical grain size will show loss in mechanical properties depends on their thickness-to grain size ratio. In fact, even those specimens that can be expected to behave as "bulk materials" on the grounds of their dimensions can undergo considerable losses of mechanical properties if their grain size becomes large enough.

Although the Hall–Petch relation, as has already been said, was initially introduced to relate the lower yield stress of a material to its grain size, it can also be used to correlate the flow stress required for different levels of strain [21]. These flow stresses can be read off from the stress–strain curves and the resulting values can be plotted as a function of the Hall–Petch parameter $D_s^{-1/2}$. Fig. 7 shows the amounts of stress required to deform the 4 mm thick specimens to a variety of strain levels ranging between 0.2 and 11%.

The results for the lower strain levels strongly suggest that the data do indeed conform to the Hall–Petch equation for the smallest grain sizes. However, a loss of strength is quite noticeable for the largest grain sizes, specially for the higher strain levels. The dotted lines represented in Fig. 7 for each strain level correspond to the Hall–Petch equation and the solid lines to its combination with a decreasing exponential term with a horizontal asymptote at the stress value where $t/D_s = 10$, above which specimen thickness seems to have no influence on mechanical properties [23].

Thus the following model results:

$$\sigma_{\text{flow}} = \sigma_0 + k_1 {D_s}^{-1/2} - \sigma_1 e^{-C((t/D_s)/((t/D_s)_{crit}))^{-1/2}} \tag{2}$$

This equation reduces to the Hall–Petch relation for bulk materials while additionally allows one to estimate the loss of strength in thin components, the behavior of which is markedly thickness-dependent. The transition occurs at a point not dependent on any intrinsic property of the material but rather, almost exclusively, on the t/D_s ratio of the particular specimen. Thus, it can occur in specimens as thin as 150 μm [17] or as thick as 4 mm depending on the grain size of the target specimen. Table 2 shows the σ_0, k_1, σ_1, y C values obtained from the fitted curves, where, for our particular case, $(t/D_s)_{crit} = 10$, as depicted in Fig. 7.

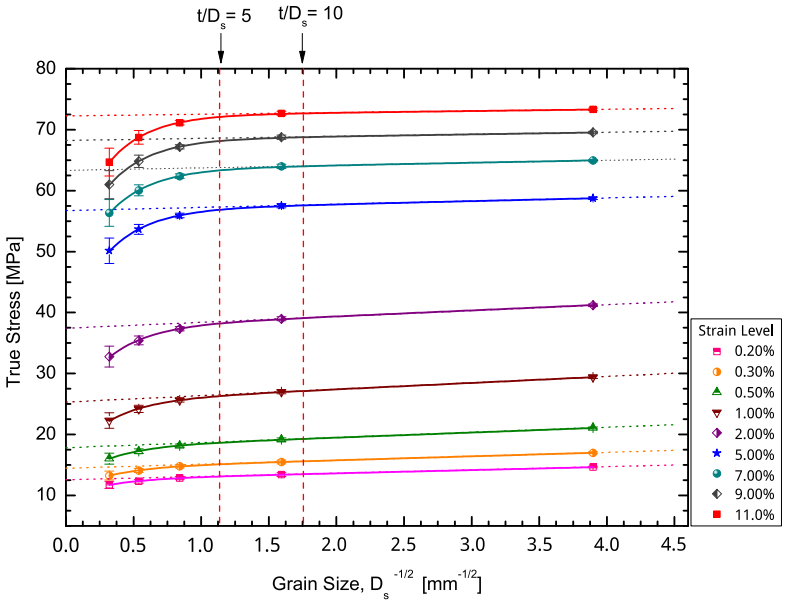

Fig. 7. Amount of stress required to cause variable levels of deformation as a function of the Hall–Petch parameter $D_s^{-1/2}$. Samples' thickness: 4 mm.

Table 2
Hall–Petch constants for aluminium alloy 1050 with $(t/D_s)_{crit} = 10$. Data derived from samples 4 mm thick.

Strain [%]	σ_0 [MPa]	k_1 [MPa m$^{1/2}$]	σ_1 [MPa]	C
0.2	12.57	0.53	3.21	2.72
0.3	14.47	0.65	4.32	2.92
0.5	17.83	0.83	6.06	3.03
1.0	25.31	1.05	9.54	3.38
2.0	37.44	0.97	13.37	3.78
5.0	56.72	0.52	17.53	4.41
7.0	63.32	0.42	18.91	4.65
9.0	68.24	0.33	19.64	4.75
11.0	72.25	0.27	20.89	4.95

A comparison of our results with those for thin films, for which the t/D_s values are similar to those studied here, reveals that the figures previously reported by Keller et al. [25] for nickel, which were fitted to two different Hall–Petch lines, can also be fitted to Eq. (2) (see Fig. 8).

3.1.3. Influence of specimen thickness

We examine now the influence of the thickness of the specimen upon mechanical properties, bearing in mind that we move in the region where thickness and grain size are of comparable magnitude. Fig. 9 shows the stress–strain curves obtained for specimens 1, 2 and 4 mm thick made of the same material with a grain size of 1.4 mm. It can be seen that increasing thickness moves the curves upward in the plastic region. Of course, this is somehow expected, as grains in the thinner specimens here are much less constrained and can deform more easily, requiring thus less stress for the same overall strain than in the thicker specimens.

Fig. 9 also shows the flow stress needed to deform the material by 5% as a function of the Hall–Petch parameter $D_s^{-1/2}$ for the three thicknesses and several grain sizes. As can be seen, when the thicknesses were much greater than grain size (D_s = 0.066 mm, corresponding to $D_s^{-1/2}$ = 3.89 in the graph) the stress value (58 MPa) was virtually the same for the three thicknesses, reflecting a typical behavior of materials experiencing no lack of constraint or edge effect. However, as the grain size increases with respect to the thickness, there is a clear departure from the possible Hall–Petch straight line and the smaller the thickness the greater the deviation. The lines drawn in this figure correspond to Eq. (2) with $(t/D_s)_{crit}$ = 10 as stated before. The values for the needed parameters are those determined previously for the 4 mm thick specimens and can be read off Table 2 for 5% strain.

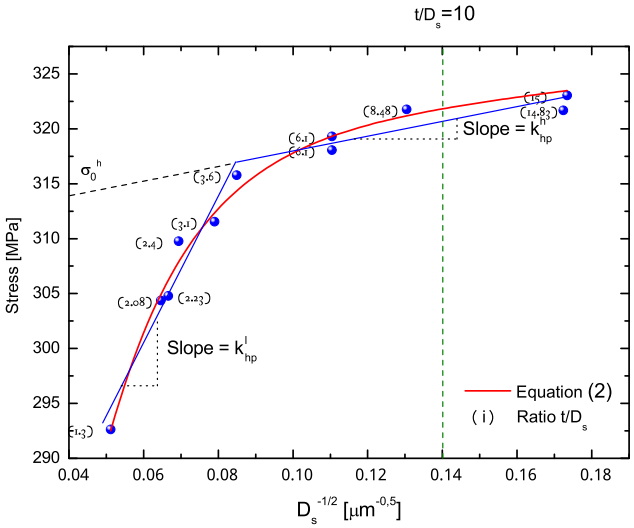

Fig. 8. Data by Keller et al. [25] fitted to two Hall–Petch lines and also to Eq. (2).

It should be borne in mind that mechanical properties were fitted with respect to the surface grain size (D_s) only. It could be argued, given the data shown in Fig. 4, that for thicker specimens a more useful definition of the representative grain size might involve some kind of average between the grain size as measured in the surface and as measured across the thickness. This has not been attempted here, but this considerations could explain why the lines drawn in the lower part of Fig. 9 for the two thinner specimens, using Eq. (2) with the parameters fitted from the thickest specimen, seem to run a little above the experimental values.

3.2. Fatigue properties

We focus now on fatigue properties, in particular endurance limit and notch sensitivity. Several S–N diagrams were obtained. The following list summarizes some key points of the experimental procedure, which is fully described in [55]:

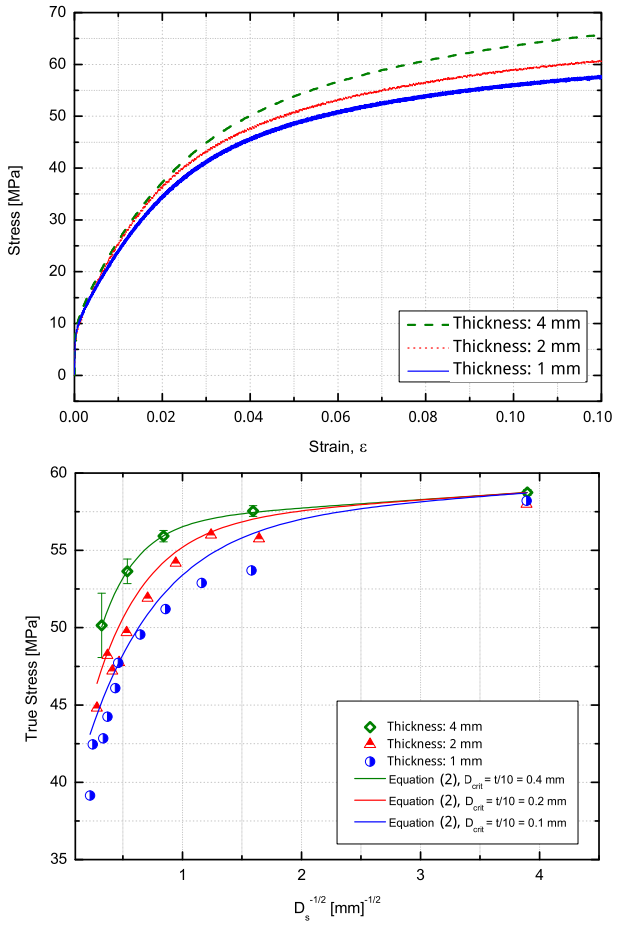

Fig. 9. Variation of mechanical properties with specimen thickness.
(a) Stress–strain curves for specimens 1, 2 and 4 mm thick made of the same material with a grain size of 1.4 mm
(b) Flow stress needed to deform the material by 5% as a function of the Hall–Petch parameter $D_s^{-1/2}$ for the three thicknesses and several grain sizes.

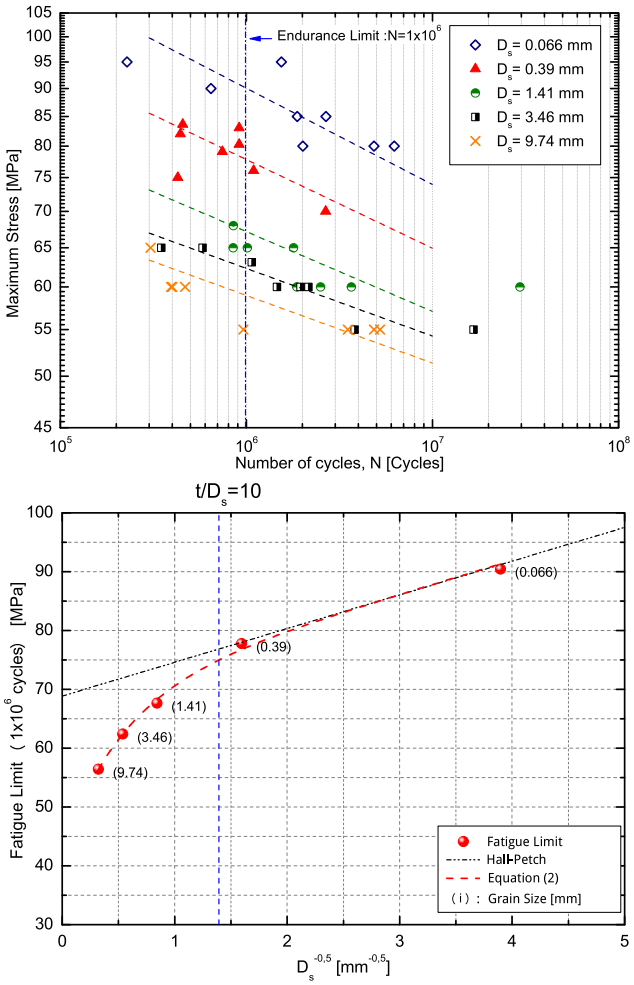

Fig. 10. (a) Unnotched S–N curves obtained for each grain size. The vertical line marks the reference for the endurance or fatigue limit, set at 1×10^6 cycles. (b) Variation with the Hall–Petch parameter $D_s^{-1/2}$.

- Specimens of five different grain sizes were used (0.066 - 0.39 - 1.41 - 3.46- 9.74 mm).
- For each grain size, a series of through the thickness circular notches of increasing radii were machined, spanning a very wide range of notch-size to grain-size ratios, from 0.2 to just over 60.
- For each of the grain sizes listed above, three sets of specimens with different notch radii of 1, 2 and 4 or 6 mm, plus the set corresponding to the plain, unnotched, condition were cut. Accordingly, up to 20 S–N diagrams were obtained for the 20 different notch-size to grain-size ratios realized.
- At least 10 specimens were tested for each S–N diagram, totaling more than 200 fatigue tests.

3.2.1. *Fatigue strength of unnotched plates*

Fig. 10(a) shows the unnotched S–N curves obtained for each grain size, as well as the corresponding linear regression curves calculated in accordance with ASTM E739 2006 (“Statistical Analysis of Linear or Linearized Stress-Life ($S-N$) and Strain-Life ($\varepsilon-N$) Fatigue Data”). The specimen thickness is 4 mm for all the test reported in this section. Because the target material was commercially pure aluminium, the S–N curves exhibited no well-defined fatigue limit (i.e., no horizontal asymptote as the test stress was decreased). Rather, they were straight lines of negative slope. This led us to consider, for the sake of comparisons, an endurance limit corresponding to the stress needed to cause failure at 1×10^6 cycles (vertical line in the graph). Although the different regression lines were extrapolated to more and fewer cycles than the experimental values in order to better illustrate the outcome, calculating the endurance limit required no extrapolation since the experimental data spanned a range including values on both sides of the chosen number of cycles (1×10^6). For the smaller grain sizes (0.066 and 0.39 mm) and for the unnotched specimens, after performing the second mechanical treatment (see Fig. 5) the elastic limit was again increased up to 90–95 MPa in order to remain within the elastic range during the fatigue tests.

Similarly to the static case, deviation of the fatigue strength from the Hall–Petch line at $t/D_s < 10$, is clearly observed, see Fig. 10(b). Despite the fact that all “materials” (different grain size) have the same chemical composition, and the same inclusions density, since they all come from the same aluminium plate, a big difference is observed in the endurance limit.

These graphs are crucial to understand the behavior of specimens with dimensions comparable to grain size where edge effects should be more noticeable. As in the static case, the material loses mechanical properties (the endurance limit, in this case) with a decrease in t/D_s. Therefore, the size effects are related not to specimen size alone, but also to the relationship between specimen dimensions and grain size. Potential critical thresholds for the characteristic dimensions above which edge effects cause loss of mechanical properties seem meaningless unless they are related to microstructural data. Here, we have a specimen with a respectable thickness of 4 mm which, nevertheless,

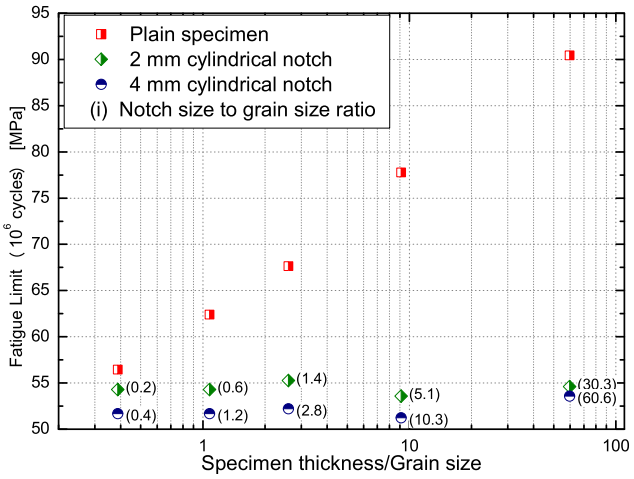

Fig. 11. Variation of the fatigue strength as a function of the t/D_s ratio. Samples' thickness: 4 mm.

shows an appreciable loss in fatigue strength when the ratios between the thickness and the grain size reach comparable values. This effect has been reported for thin films by several authors [6,13,23–25], mainly working with tensile properties.

3.2.2. Fatigue strength of notched plates

Next the question of whether the behavior of notched specimens is also affected by edge effects or not is examined. This obviously requires that the size of the notch relative to both the specimen thickness and grain size be brought into the analysis.

Fig. 11 shows the fatigue limit (endurance, as explained above) for five different grain sizes in unnotched specimens as well as in notched specimens with a circular hole of 2 and 4 mm in diameter. As can be seen, whereas the endurance limit for the unnotched specimens is greatly influenced by the thickness-to-grain size ratio, this does not seem to be the case for the notched specimens. The notched endurance limits obtained for each of the two hole diameters remain almost constant, irrespective of the grain size. While the plain endurance limits seems to fall nicely in a linear relationship with respect to the ratio between thickness and grain size (log), the notched endurances do not change as much.

However, the notched fatigue strength seems to be influenced by the size of the notch, for doubling the diameter of the hole consistently reduces endurance limits by about 5%. This is clear, at least for the cases where the notch is smaller than the grain size and up to notch sizes of around 10 grains. Note also, that, as one would expect, when the notch is much bigger than the microstructure, the size of the notch itself ceases to be so determinant and the fatigue strengths obtained for the 2 and 4 mm notches for the smallest grain size are closer. This is, of course, our own interpretation of the data. It may be felt that there are not enough points to support this last claim and that some more points for ratios between 10 and, say, 50, would be needed. And we gladly admit this. Needless to say, we did not foresee this need when the experiments were first planned and tests in that region could not be carried out later for various reason. Note that each point in Fig. 11 represents really a whole S–N curve, so that the total number of fatigue experiments that went into the figure is around 200, as has already been mentioned.

It seems, therefore, that, in the present experiments, the notch effect is as strong as the edge effect. The relative proximity in the figure of the unnotched and notched strengths for the biggest grain size and the steady and fast separation when the grains get smaller and the specimens get thicker does, of course, agree, with the classical ideas on *notch sensitivity*.

It is well known that the fatigue limit of notched specimens is usually higher than that calculated by dividing the plain-specimen fatigue limit by the theoretical stress concentration factor given by the theory of elasticity. Thus K_f, the so-called *fatigue notch factor*, defined as the ratio between the fatigue limit of specimens with no stress concentration and the fatigue limit of specimens with a stress raiser, is usually smaller than the elastic stress concentration factor K_t. This effect seems to depend both on the notch geometry and on the material. Specimens with the same geometry and dimensions but made of different materials have varying fatigue notch factors. Some materials are more sensitive to the presence of a notch than others [56, p. 13] and the *notch sensitivity index* is introduced to measure the material's sensitivity to stress concentration [57, p. 9]:

$$q = \frac{K_f - 1}{K_t - 1} \tag{3}$$

This provides a scale of notch sensitivity which varies from $q = 0$ or *no notch effect*, i.e., $K_f = 1$, to $q = 1$ or *full notch effect*, when $K_f = K_t$.

Different theories have been advanced to account for notch sensitivity. Two of the best known are those based on the work of Neuber (1946) [58] and of Peterson (1959) [59]. Both use the idea of a certain characteristic distance (a material constant representing an 'elementary block unit' of material) and both argue that if fatigue failure is to occur, either the average stress over this block (Neuber) or the value of the stress at a depth below the notch surface equal to the characteristic dimension of this block unit (Peterson), must equal the plain fatigue limit of the material. In the case of Peterson, the following simple formula is derived

$$q = \frac{1}{1 + a/r} \tag{4}$$

where a is a material constant (with dimensions of length) and r is notch tip radius. The constant a can be obtained by fitting experimental data comparing fatigue strengths of smooth and notched specimens of known K_t and notch radius and it has been found to depend upon the ultimate tensile strength S_u and, thus, upon the grain size. For example, the SAE Fatigue Design Handbook [60, p. 296] and the ASM Fatigue and Fracture Handbook [61, p. 242] provide the following empirical relationship:

$$a(\text{mm}) = 0.0254 \left(2079(\text{MPa})/S_u(\text{MPa})\right)^{1.8} \tag{5}$$

to estimate a in the case of steels. To the best of our knowledge, no relationship of this type exists for aluminium alloys, but the same general principles should apply.

It can be seen that the trends predicted with Eqs. (4) and (5) are in accordance with the behavior found experimentally. For example, Peterson [59] reported that for coarse grain materials, such as annealed or normalized steels, the values found for q are usually well below one, and only approach one for the larger notches. On the other hand, for fine grain materials, such as quenched and tempered steels, the values obtained for q, are very near one, sometimes fractionally below or above, due to the inherent large scatter in the experimental results.

Please see [62,63] for a further discussion of the interrelation between notch sensitivity and microstructure within the context of a short crack growth model.

Thus, in our notched specimens, what we see is that increasing grain size has two opposing effects, namely: a decrease in the plain endurance limit associated with the decrease in thickness relative to grain size and an increase in notched fatigue strengths brought about by a decrease in notch sensitivity, the net effect being that the notched fatigue strengths shown in Fig. 11 remains fairly constant.

4. Conclusions

Previously reported data, and experimental results obtained in this work, allow us to state that the size effect is not solely governed by specimen size but rather by the ratio of specimen dimensions to

grain size. The critical thresholds of the characteristic dimensions above which edge effects cause a material to lose mechanical properties are meaningless in the absence of microstructural data. Thus, a film a few tens of a micron thick may or may not undergo a decline in mechanical properties depending on its grain size. Likewise, a sheet 4 mm thick, which should normally behave as a bulk material in terms of yield stress, fracture strain or fatigue endurance can have its mechanical properties substantially diminished at a low enough characteristic dimension-to-grain size ratio.

Operating at $t/D_s > 1$ not necessarily means that grains will span the whole specimen thickness. In fact, increasing grain size by using the proposed growth technique caused D_s to depart from its proportional relation to D_t to an extent such that $D_s > t > D_t$. Therefore, the microstructure of a microcomponent cannot be fully explained in terms of surface grain size alone.

For more accurate characterization, the Hall–Petch relation can be expanded with an exponential term dependent on the t/D_s ratio. The new term is zero at high enough t/D_s values but gains significance as grain size approaches specimen thickness — and edge effects become substantial and lead to a decline in mechanical properties. The fact that the exponential term depends on t/D_s rather than on specimen thickness alone allows the decline to be assessed via single term.

The S–N curves obtained in fatigue tests for unnotched, plain components revealed a strong influence of specimen thickness; also, the fatigue limit obeyed a relation similar to the static relation between yield stress and t/D_s.

Notched components cannot be fully characterized by examining the influence of the specimen thickness-to-grain size ratio alone; in fact, they require additionally analyzing the effect of the notch size-to-grain size ratio on fatigue life.

Declaration of competing interest

The authors declare that they have no known competing financial interests or personal relationships that could have appeared to influence the work reported in this paper.

Acknowledgments

The authors would like to thank the European Union, the Spanish Government and the Junta de Andalucía, Spain for its financial support through grants PID2020-117407GB-I00 (FEDER/Ministerio de Ciencia e Innovación - Agencia Estatal de Investigación) and P18-FR-4306 (“Fondo Europeo de Desarrollo Regional (FEDER) *y* Consejería de Economía, Conocimiento, Empresas *y* Universidad de la Junta de Andalucía, dentro del Programa Operativo FEDER 2014-2020”).

References

[1] Everett KD, Conway C, Desany GJ, Baker BL, Choi G, Taylor CA, et al. Structural mechanics predictions relating to clinical coronary stent fracture in a 5 year period in FDA MAUDE database. Ann Biomed Eng 2016;44:391–403.
[2] US Food and Drug Administration (FDA). Non-clinical engineering tests and recommended labeling for intravascular stents and associated delivery systems - guidance for industry and FDA staff. U.S. Department of Health and Human Services, Food and Drug Administration, Center for Devices and Radiological Health, Interventional Cardiology Devices Branch, Peripheral Vascular Devices Branch, Division of Cardiovascular Devices, Office of Device Evaluation; 2010.
[3] Auricchio F, Constantinescu A, Conti M, Scalet G. A computational approach for the lifetime prediction of cardiovascular balloon-expandable stents. Int J Fatigue 2015;75:69–79.
[4] Auricchio F, Constantinescu A, Conti M, Scalet G. Fatigue of metallic stents: From clinical evidence to computational analysis. Ann Biomed Eng 2016;44:287–301.
[5] Connolley T, Mchugh PE, Bruzzi M. A review of deformation and fatigue of metals at small size scales. Fatigue Fract Eng Mater Struct 2005;28:1119–52.
[6] Arzt E. Size effects in materials due to microestructural and dimensional constrains: A comparative review. Acta Metall 1998;46(16):5611–26.
[7] Fleck NA, Hutchinson JW. A phenomenological theory for strain gradient effects in plasticity. J Mech Phys Solids 1993;41(12):1825–57.
[8] Fleck NA, Muller GM, Ashby MF, Hutchinson JW. Strain gradient plasticity: theory and experiment. Acta Metall Mater 1994;42(2):475–87.
[9] Fredriksson P, Gudmundson P. Size-dependent yield strength of thin films. Int J Plast 2005;21(9):1834–54.
[10] Klusemann B, Svendsen B, Vehoff H. Investigation of the deformation behavior of Fe-Si sheet metal with large grains via crystal plasticity and finite-element modeling. Comput Mater Sci 2012;52(1):25–32.
[11] Henning M, Vehoff H. Local mechanical behavior and slip band formation within grains of thin sheets. Acta Mater 2005;53(5):1285–92.
[12] Henning M, Vehoff H. Statistical size effects based on grain size and texture in thin sheets. Mater Sci Eng A 2007;452–453:602–13.
[13] Klein M, Hadrboletz A, Weiss B, Khatibi G. The size effect on the stress-strain, fatigue and fracture properties of thin metallic foil. Mater Sci Eng 2001;A319-321:924–8.
[14] Hadrboletz A, Weiss B, Khatibi G. Fatigue and fracture properties of thin metallic foils. Int J Fract 2001;109:69–89.
[15] Murphy BP, Savage P, McHugh PE, Quinn DF. The stress-strain behaviour of coronary stent struts is size dependent. Ann Biomed Eng 2003;31:686–91.
[16] Rooein M. Investigation of the structure - property - processing relationships of 316L stainless steel hypotubing (Masters thesis), San José State University; 1995.
[17] Weiss B, Gröger V, Khatibi G, Kotas A, Zimprich P, Stickler R, et al. Characterization of mechanical and thermal properties of thin Cu foils and wires. Sensors Actuators A 2002;99(1–2):172–82.
[18] Lederer M, Gröger V, Schafler E. The influence of the texture on yield strength and strain hardening of high purity aluminum foils. Arch Metall Mater 2008;53(1):69–73.
[19] Hall EO. The deformation and ageing of mild steel-III discussion of results. Proc Phys Soc Ser B 1951;64:747–53.
[20] Petch NJ. The cleavage strength of polycrystals. J Iron Steel Inst 1953;174:25.
[21] Conrad H, Schoeck G. Cottrell locking and the flow stress in iron. Acta Metall 1960;8(11):791–6.
[22] Pell-Walpole WT. The effect of grain-size on tensile strength of tin and tin alloys. J Inst Metals 1943;69:131–46.
[23] Miyazaki S, Shibata K, Fujita H. Effect of specimen thickness on mechanical properties of polycrystalline aggregates with various grain sizes. Acta Metall 1978;27:855–62.
[24] Janssen PJM, de Keijser TH, Geers M. An experimental assessment of grain size affects in the uniaxial straining of thin al sheet with a few grains across the thickness. Mater Sci Eng A 2005;419(16):238–48.
[25] Keller C, Hug E. Hall-Petch behaviour of Ni polycristals with a few grains per thickness. Mater Lett 2008;62:1718–20.
[26] Hug E, Keller C. Intrinsic effects due to the reduction of thickness on the mechanical behavior of nickel polycrystals. Metall Mater Trans A 2010;41:2498–506.
[27] Keller C, Hug E, Feaugas X. Microstructural size effects on mechanical properties of high purity nickel. Int J Plast 2011;27:635–54.
[28] Keller C, Hug E, Habraken AM, Duchene L. Finite element analysis of the free surface effects on the mechanical behavior of thin nickel polycrystals. Int J Plast 2012;29:155–72.
[29] Fu H-H, Benson DJ, Meyers MA. Analitical and computational description of effect of grain size on yield stress of metals. Acta Mater 2001;49:2567–82.
[30] Lederer M, Gröger V, Khatibi G, Weiss B. Size dependency of mechanical properties of high purity aluminum foils. Mater Sci Eng A 2010;527:590–9.
[31] Zhang G, Volkert C, Schwaiger R, Mönig R, Kraft O. Fatigue and thermal fatigue damage analysis of thin metal films. Microelectron Reliab 2007;47(12):2007–13.
[32] Dai CY, Zhang GP, Yan C. Size effects on tensile and fatigue behaviour of polycrystalline metal foils at the micrometer scale. Phil Mag 2011;91(6):932–45.
[33] Simons G, Weippert C, Dual J, Villain J. Size effects in tensile testing of thin cold rolled and annealed Cu foils. Mater Sci Eng A 2006;416(1–2):290–9.
[34] Hong S, Weil R. Low cycle fatigue of thin copper foils. Thin Solid Films 1996;283(1–2):175–81.
[35] Read D. Tension-tension fatigue of copper thin films. Int J Fatigue 1998;20(3):203–9.
[36] Agnew S, Weertman JR. Cyclic softening of ultrafine grain copper. Mater Sci Eng A 1998;244:145–53.
[37] Schwaiger R, Kraft O. Size effects in the fatigue behavior of thin Ag films. Acta Mater 2003;51(1):195–206.
[38] Khatibi G, Betzwar-Kotas a, Groger V, Weiss B. A study of the mechanical and fatigue properties of metallic microwires. Fatigue Fract Eng Mater Struct 2005;28(8):723–33.
[39] Zhang J, Jiang Y. Fatigue of polycrystalline copper with different grain sizes and texture. Int J Plast 2006;22(3):536–56.
[40] Zhang G, Takashima K, Higo Y. Fatigue strength of small-scale type 304 stainless steel thin films. Mater Sci Eng A 2006;426(1–2):95–100.
[41] Zhang G, Volkert C, Schwaiger R, Wellner P, Arzt E, Kraft O. Length-scale-controlled fatigue mechanisms in thin copper films. Acta Mater 2006;54(11):3127–39.
[42] Dai C, Zhang B, Xu J, Zhang G. On size effects on fatigue properties of metal foils at micrometer scales. Mater Sci Eng A 2013;575:217–22.

[43] Kim C-Y, Song J-H, Hwangbo Y, Shim H-S. Plastic deformation behavior of Cu thin films during fatigue testing. Procedia Eng 2010;2(1):1421–30.
[44] Tanaka K, Sakakibara M, Kimachi H. Grain-size effect on fatigue properties of nanocrystalline nickel thin films made by electrodeposition. Procedia Eng 2011;10:542–7.
[45] Liew LA, Read DT, Barbosa N. MEMS-based universal fatigue-test technique. Exp Mech 2012;53(5):783–94.
[46] Lee D-Y, Song J-H. Fatigue life and plastic deformation behavior of electrodeposited copper thin film under variable amplitude loading. Int J Fatigue 2012;38:1–6.
[47] Baumert EK, Sadeghi-Tohidi F, Hosseinian E, Pierron ON. Fatigue-induced thick oxide formation and its role on fatigue crack initiation in Ni thin films at low temperatures. Acta Mater 2014;67:156–67.
[48] Wiersma S, Taylor D. Fatigue of materials used in microscopic components. Fatigue Fract Eng Mater Struct 2005;28(12):1153–60.
[49] Carpenter HCH, Elam CF. Recystallization in metals. J Inst Metals 1920;24:83–131.
[50] Carpenter HCH, Elam CF. The production of single crystals of aluminium and their tensile properties. Proc R Soc Lond 1921;100(704):329–53.
[51] Lorenzino P. Fatiga en componentes con concentradores de tensión bajo carga en modo I (Ph.D. thesis), Seville University; 2012.
[52] Lorenzino P, Navarro A, Krupp U. Naked eye observations of microstructurally short fatigue cracks. Int J Fatigue 2013;56:8–16.
[53] Lorenzino P, Navarro A. The variation of resonance frequency in fatigue tests as a tool for in-situ identification of crack initiation and propagation, and for the determination of cracked areas. Int J Fatigue 2015;70:374–82.
[54] Lorenzino P, Navarro A. Growth of very long "short cracks" initiated at holes. Int J Fatigue 2015;71:64–74.
[55] Lorenzino P, Navarro A. Grain size effects on notch sensitivity. Int J Fatigue 2015;70:205–15.
[56] Duggan TV, Byrne J. Fatigue As a Design Criterion. London: Macmillan Education UK; 1977.
[57] Peterson R. Stress concentration factors: charts and relations useful in making strength calculations for machine parts and structural elements. Wiley; 1974.
[58] Neuber H. Kerbspannungslehre. Springer Verlag; 1937, translated into English, Theory of Notches, Edwards, J. W., Ann Arbor, MI, 1946.
[59] Peterson RE. Notch sensitivity. In: Sines G, Waisman JL, editors. Metal fatigue. McGraw-Hill; 1959, p. 293–307.
[60] Socie D, Reemsnyder H, Downing S, Tipton S, Leis B, Nelson D. Chapter 10 Fatigue life prediction. In: Rice RC, editor. SAE Fatigue design handbook, AE-22. 3rd Ed.. Society of Automotive Engineers, Warrendale, PA; 1997, p. 285–382.
[61] Mitchell MR. Fundamentals of modern fatigue analysis for design. In: Lampman SR, editor. ASM Handbook volume 19: Fatigue and fracture, section 3: Fatigue strength prediction and analysis. ASM International. Material Park, OH; 1996, p. 227–49.
[62] Navarro A, Vallellano C, de los Rios ER, Xin XJ. Notch sensitivity and size effects described by a short crack propagation model. In: Beynon JH, Brown MW, Smith RA, Lindley TC, Tomkins B, editors. Engineering against fatigue. Balkema Publishers; 1997, p. 63–72.
[63] Chaves V, Navarro A. Application of a microstructural model for predicting notch fatigue limits under mode I loading. Int J Fatigue 2009;31(5):943–51.